IEEE Access
Multidisciplinary ⋮ Rapid Review ⋮ Open Access Journal

Received 14 March 2023, accepted 6 April 2023, date of publication 13 April 2023, date of current version 19 April 2023.

*Digital Object Identifier 10.1109/ACCESS.2023.3266771*

APPLIED RESEARCH

# Prediction of Survival of Glioblastoma Patients Using Local Spatial Relationships and Global Structure Awareness in FLAIR MRI Brain Images

**MINH-TRIEU TRAN, HYUNG-JEONG YANG, (Member, IEEE), SOO-HYUNG KIM, (Member, IEEE), AND GUEE-SANG LEE, (Member, IEEE)**
Department of Artificial Intelligence Convergence, Chonnam National University, Gwangju 61186, South Korea

Corresponding author: Guee-Sang Lee (gslee@jnu.ac.kr)

This work was supported in part by the Basic Science Research Program through the National Research Foundation of Korea (NRF) funded by the Ministry of Education under Grant NRF-2018R1D1A3B05049058, and in part by the Bio and Medical Technology Development Program of the NRF funded by the Korean Government [Ministry of Science and ICT (MSIT)] under Grant NRF-2019M3E5D1A02067961.

**ABSTRACT** This article introduces a framework for predicting the survival of brain tumor patients by analyzing magnetic resonance images. The prediction of brain tumor survival is challenging due to the limited size of available datasets. To overcome the issue of overfitting, we propose a self-supervised learning method that involves identifying image patches from the same or different images. By recognizing intra- and inter-image differences, the network can learn the relationships between local spatial windows in the same image and across different images. In addition to analyzing local information, we also incorporate a global structure awareness network to capture global information from the entire image. Our proposed method shows a strong correlation between local spatial relationships and survivor class prediction in FLAIR MRI brain images. We evaluate our method using the BraTS 2020 validation dataset and observe that our method outperforms others in accuracy and SpearmanR correlation metrics.

**INDEX TERMS** Brain tumor, survival prediction, local context, global structure, deep learning.

## I. INTRODUCTION

Glioblastoma is considered to be one of the most dangerous brain tumors, because it has a poor prognosis. Oncologists divide patients with brain tumors into three classes: short, mid-term, and long survivor [1]. Early classification can help extend the lifetime of brain tumor patients by facilitating appropriate treatment. According to MR images, there are three kinds of brain tumor regions: edema tumors, necrotic tumors, and enhancing tumors. Each patient has a different survival time depending on a variety of factors related to their kind of brain tumors themselves. Therefore, the MRI analysis of brain tumors is essential to the planning of treatment. Local spatial information may be valuable [2], [3], [4], [5], [6], [7], [8] such as peritumoral area, surrounding mass, and the contact between the tumor and the ventricle. We believe that local spatial relationships in MRI brain images can assist in the understanding of brain structure and lead to improved prediction of survival times. Additionally, many papers [9], [10], [11], [12], [13] about the global structure of the brain has proven its correlation with survival prediction in glioblastoma patients. Firstly, the disruptions in the normal-appearing brain beyond the lesion could mediate the topological alteration of the connectome associated with worse patient survival [9]. Secondly, disruptions in brain networks caused by a stroke can lead to post-stroke depression, which is a common complication. These disruptions are also related to the prediction of survival outcomes in patients with glioblastoma [10], [11]. The impact of glioblastoma on global brain function, including functional communication between brain regions far from the tumor, has been carefully investigated in previous research [12]. Finally, neuroplasticity of structural, topological, biochemical metabolism, and related mechanisms of the brain come through multimodal MRI [13],

The associate editor coordinating the review of this manuscript and approving it for publication was Kah Phooi (Jasmine) Seng.

which may contribute to the improvement of prognosis and function in glioma patients. Based on the valuable global structure information with prognosis in glioblastoma patients, as we mentioned, we therefore integrated knowledge about the global structure as an embedding feature vector in our survival prediction network.

The main contributions of this paper can be summarized as follows:

- We propose a framework for the prediction of survivor class based on local spatial relationships in FLAIR MRI data from patients with brain tumors to capture the medical characteristic related to survival prediction relying on deep feature information. The local areas are helpful for survival prediction in GBM because they could be contained critical information, such as the growing tumor, surrounding mass effect, and the status of tumor contact with the ventricle and stromal cells that promote GBM growth and invasion.
- Global structures of the brain have proven their correlation with survival prediction in glioblastoma patients, so we employed a global structure awareness network to capture global information from an entire image and then use it for the survival prediction task.
- We show that exploiting a combination of local and global information in FLAIR images can improve the prediction of survival in brain tumor patients.
- In experiments, we achieved an accuracy of 62.1 % and a Spearman R correlation of 0.576. Our proposed method outperformed other state-of-the-art methods.
- We believe that the proposed method can efficiently support doctors and oncologists in determining the prognoses of brain tumor patients.

## II. RELATED WORKS

Computer-aided prediction of survival times for patients with brain tumors is important to oncologists, and has been the subject of considerable research. There are two main approaches. The first approach is the use of radiomic feature extraction, while the second uses other features, such as context features, instead of radiomics features.

In the first approach, radiomics features are used for the prediction of survival. Several researchers [14], [15], [16], [17], [18], [19], [20] have used the BraTS dataset for training and evaluation. Deep features combined with radiomic (intensity, texture, wavelet, shape) and clinical information, are initially used, and then those features are input into a random forest regressor [14] to predict overall survival in days. One approach [15] employed a combination of radiomics features to train a linear regressor for survival prediction. These researchers used volume and surface features from three kinds of tumors, together with age information. Another study used 4524 radiomics features and clinical data to train a random forest regressor [16]. Location features were investigated in [17] using a fusion of radiomics, location, and clinical features. A multilayer perceptron (MLP) network was then used for survival prediction using 13 shape features and clinical information [18]. Instead of using Cox proportional hazards, [19] employed support vector machines in a survival prediction network, using 81 shape radiomics features. The ratio of tumor size to brain size, area of tumor surface, and clinical features were used to train an MLP survival prediction network in [20].

However, when we used radiomics features, the model tended to overfit. The use of radiomics features requires a large-scale dataset; the number of patients should be at least ten times that of the radiomics features extracted [21], [22], [23].

In order to solve those problems, many researchers have used dimensional reduction methods to decrease the number of radiomics features. The remaining features are more closely correlated to the survival information. Additionally, radiomics features are very sensitive to the intensities in the images [22].

A method for forecasting patient survival, which combines MobileNet with a linear survival prediction model (SPM), is outlined in [24]. Different versions of MobileNet are assessed to identify the most effective one, including adapting MobileNet V1 with either frozen or unfrozen layers and modifying MobileNet V2 with either frozen or unfrozen layers connected to SPM. The research employed the BraTS 2020 dataset. Based on the findings of the experiment, a modification of MobileNet V2 architecture that included frozen layers was chosen. The authors of [25] utilized the DeepSCAN framework, which achieved impressive results in the 2019 BraTS challenge and was trained with an uncertainty-aware loss, to sort cases into two groups: those with a precisely segmented core and those with an ambiguously segmented or absent core. Assuming that every tumor has a core, they decreased the classification threshold for core tissue in cases where the model's core classification was unclear or missing. They subsequently employed a combination of linear regression and random forest classification to predict the survival of high-grade glioma patients, taking into account variables such as age, number of distinct tumor components, and number of unique tumor cores. In [26], a combination of radiomic and image-based features were utilized to forecast the overall survival time of patients. Initially, automatic segmentation of gliomas from brain MRI volumes is crucial to detect tumors. Previous research has proposed various 2D Convolutional Neural Network (2D-CNN) and 3D-CNN based architectures, which are employed to capture contextual information. The 3D models capture depth information, making them suitable for glioma segmentation from 3D MRI images. However, 2D models can be trained more quickly, making parameter tuning simpler. To leverage the benefits of both models, the authors proposed an ensemble of 2D and 3D models. After segmentation, the OS time prediction was performed on segmented tumor sub-regions. For this purpose, multiple radiomic and image-based features were extracted from MRI volumes and segmented sub-regions.

In [27], four networks - three 2D networks for each patient plane (axial, sagittal, and coronal) and one 3D network - were combined to segment tumors from MRI images, with Dice scores of 0.75 for the enhancing tumor (ET), 0.81 for the whole tumor (WT), and 0.78 for the tumor core (TC). Using features extracted from the automatic segmentation, a survival prediction model was developed on Matlab, with gross tumor size and location being the major factors influencing survival prediction. The feature extraction was carried out on Matlab using the Image processing toolbox, resulting in numerous features extracted from the segmentation matrix and the four MRI sequences. To predict survival, the Matlab Machine Learning toolbox was employed. The use of a fully convolutional neural network for glioma segmentation on the BraTS 2019 dataset is demonstrated in [28]. A three-layers deep encoder-decoder architecture with dense connection at the encoder part is utilized to propagate information from coarse layers to deep layers. This architecture is employed to train three tumor sub-components individually, with the sub-component training weights initialized with whole tumor weights to determine the tumor's location within the brain. Three segmentation results are merged to obtain the entire tumor segmentation. The survival prediction is based on radiomic features from the segmentation results, along with age and statistical features, using random forest regressors to predict the overall survival of patients. In study [29], a modified U-Net architecture was used with appropriate normalization and patch selection methods for brain tumor segmentation in the BraTS 2020 challenge. A two-phase network training was implemented with patch selection methods. The segmentation outcome with various radiomic features was used for predicting Overall Survival (OS). Although the algorithm achieved successful OS prediction, there is still room for improvement in tumor inter-class segmentation and OS prediction using different network implementation strategies. Since the OS prediction results are based on segmentation, improving segmentation will lead to better OS prediction outcomes. The proposed approach in paper [30] is to use a neural network that consists of various building blocks to recognize the different histologic sub-regions of gliomas in multi-parametric MRIs. The model also extracts radiomic features to estimate the prognosis of a patient. This study [31] presents an automated approach for segmenting gliomas in pre-operative brain MRI scans using a 3D deep learning method. They propose a multi-resolution architecture based on an encoder-decoder model with separate branches to incorporate both local high-resolution image features and wider low-resolution contextual information. The training process utilizes a unified multi-task loss function. In addition to the segmentation task, they also introduce a regression algorithm based on random forests to predict survival days for patients. The proposed network is fully automated and designed to work with patches of any arbitrary size as input. The authors of paper [32] have developed a deep learning model named PieceNet which is an ensemble of patch-based 3D UNets. They have used uncorrected modalities to train a standard 3D UNet for all label classes and one 3D UNet for each individual label class. The results show that this 4-network ensemble technique is potentially better than traditional patch-based 3D UNet on uncorrected images, but further work is needed to improve enhancing tumor segmentation. Additionally, the authors have created a linear probability model that utilizes radiomic and non-imaging features to predict survival after surgery. From the illustration of Table 1 Our proposed method not only utilizes complete information from global, local, and radiomics features but can also be employed for the segmentation step.

We believe that self-supervised learning in brain survival classification could help to develop models which better understand the dataset and deal with the problem of small datasets. In this paper we propose a novel approach to brain tumor survival prediction partially based on self-supervised learning.

## III. PROPOSED METHOD

Recently, most methods for the prediction of survival for patients with brain tumors consist of two stages: segmentation and survival prediction. In the first stage, a segmentation framework segments tumors into necrotic, edema tumor, or enhancing tumor. Next, some feature extraction methods use segmented maps to produce feature information. A survival prediction network then uses those features for training. Our approach also consists of two stages. Figure 1 illustrates the architecture of the proposed method. Our approach includes three steps: tumor segmentation, learning the local spatial relationships, and finally, we utilize the pre-trained backbone from the second step to train the survivor class prediction network. The proposed method is an expansion of our previous method [33] which employs only the information from local spatial relationships in FLAIR MRI brain images to classify the survivor class. We recognized that the global information and radiomics features also have important roles in survival prediction. Therefore, we try to utilize the combination together of all kinds of information.

Although our approach involves two steps, our main focus is on the second step, which is survival prediction. Therefore, in the segmentation stage, we choose the models that are relatively suitable for objects of small and medium size. It is from this goal that we choose DKNet and DMFNet to handle the segmentation task. DMFNet is a lightweight network to significantly reduce the computational cost. Furthermore, this framework employed 3D dilated convolutions to build multi-scale feature representation. Additionally, DKNet is prove to have a good deal with the brain tumor segmentation of any sizes which may have a significant impact on finding early-stage cancers. Based on above reasons, we selected DKNet and DMFNet for our segmentation step.

### A. SEGMENTATION

In most of the research into survival analysis or survival prediction, segmentation is crucial for the determination of the location and size of the tumor. Brain tumor segmentation

**TABLE 1.** Comparison between our proposed method with others.

| Reference | Segmentation | Local Information | Global information | Tumor's features | |
|---|---|---|---|---|---|
| | | | | Radiomics | Non-Radiomics |
| [24] | | | ✓ | | |
| [25] | ✓ | | | | ✓ |
| [26] | ✓ | | ✓ | ✓ | |
| [27] | ✓ | | | | ✓ |
| [28] | ✓ | | | ✓ | |
| [29] | ✓ | | | ✓ | |
| [30] | ✓ | | | ✓ | |
| [31] | ✓ | | | ✓ | |
| [32] | ✓ | | | ✓ | |
| Ours | ✓ | ✓ | ✓ | ✓ | |

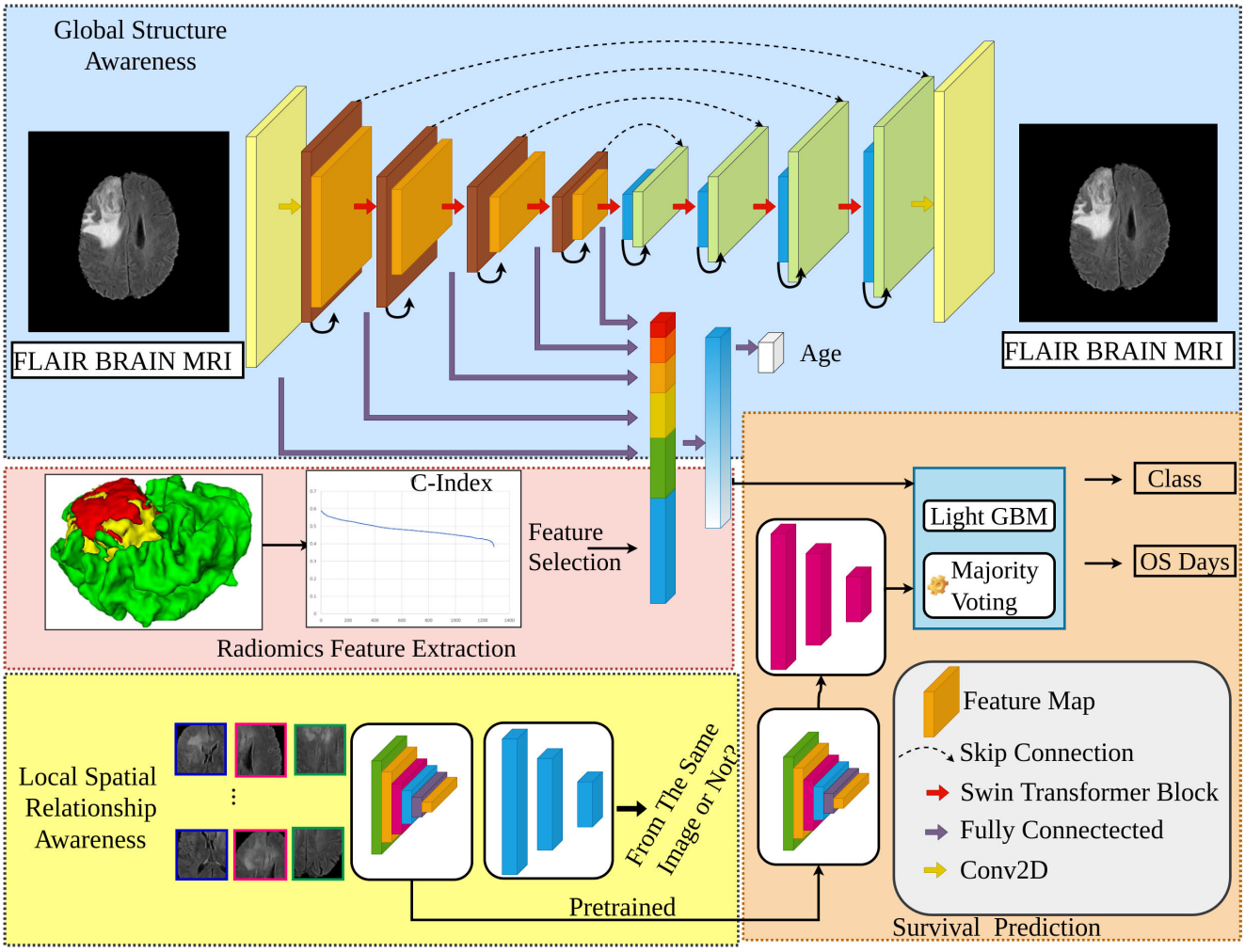


**FIGURE 1.** The architecture of the proposed method. Our approach includes three steps: The first step is tumor segmentation, The second is learning the local spatial relationships, and finally, we utilize the pre-trained backbone from the second step to train the survivor class prediction network.

of MR images is challenging because of the heterogeneity of tumors, and variations in the size and brightness of the tumor in the image. There are several papers also tackled the problem related to segmentation some important areas in the brain like [34] and [35]. In particularly, the paper [34] presents an iterative implementation of the level set methodology that aims to accurately segment normal and abnormal tissues in MRI brain images. The segmentation includes normal tissues such as white matter, grey matter, and cerebrospinal fluid, as well as other regions of the human head such as the skull, marrow, and muscle skin. Abnormal tissues like hemorrhage, edema, and tumor can also be segmented if present. The segmentation process uses an iterative three-region level set method that is based on the condition of a sharp peak greater

than three. The segmented components are iteratively generated to create a hierarchical structure for accurate segmentation. The effectiveness of the segmentation method is evaluated using various metrics, such as accuracy, similarity index, and relative error, on a defined set of MRI brain images. Additionally, this research [35] introduces a new approach using level set methodology to segment brain tissues in MRI brain images. The segmentation method includes normal tissues like WM, GM, and CSF, as well as other parts of the head like the skull, marrow, and muscular skin. The method uses repeated level set iterations based on a sharp peak condition greater than three. Each segmented component creates a hierarchical structure to ensure accurate tissue segmentation. The segmentation method's performance is evaluated using accuracy, sensitivity, and error correction metrics, and a defined set of MRI brain is used for analysis. Both visual and mathematical assessments indicate that the proposed method yields superior results for brain MR images. Besides, this article [36] examines the current paradigm in healthcare, as well as the potential for new scientific discoveries and the technological advancements that support them. It also explores the possibilities for supervised machine learning (SML) in a range of healthcare sectors, as well as the ethical concerns surrounding these developments. The article assesses the potential for disease diagnosis, personalized medicine, clinical trials, non-invasive image analysis, drug discovery, patient care services, remote patient monitoring, hospital data, and nanotechnology to benefit from learning-based automation in healthcare. Additionally, the need for explainable artificial intelligence (AI) in healthcare is emphasized. However, our primary purpose is to investigate the survival classification method. Therefore, instead of developing a new segmentation framework, we used a segmentation method based on an ensemble approach that uses two available effective deep learning models, DMFNet [37] and DKNet [38], to segment three kinds of tumors: edema, enhancing, and necrotic tumors, from brain MR images. DMFNet is a highly efficient 3D CNN using lightweight 3D convolutional networks to accurately capture multi-scale feature representations. The DKNet is a multi-tasking learning approach with feature reconstruction as an auxiliary task essential for retaining the essential features of small tumors. Figure 2 presents an overview of tumor segmentation. The proposed method uses only the FLAIR modality to extract the local and global features. Several segmentation results are shown in Figure 9. (A) column is the input images, (B) column is our segmented results, (C) column is the segmented results from DKNet, (D) column is the segmented results from DMFNet. The proposed framework for segmentation achieves better Dice scores compared to others.

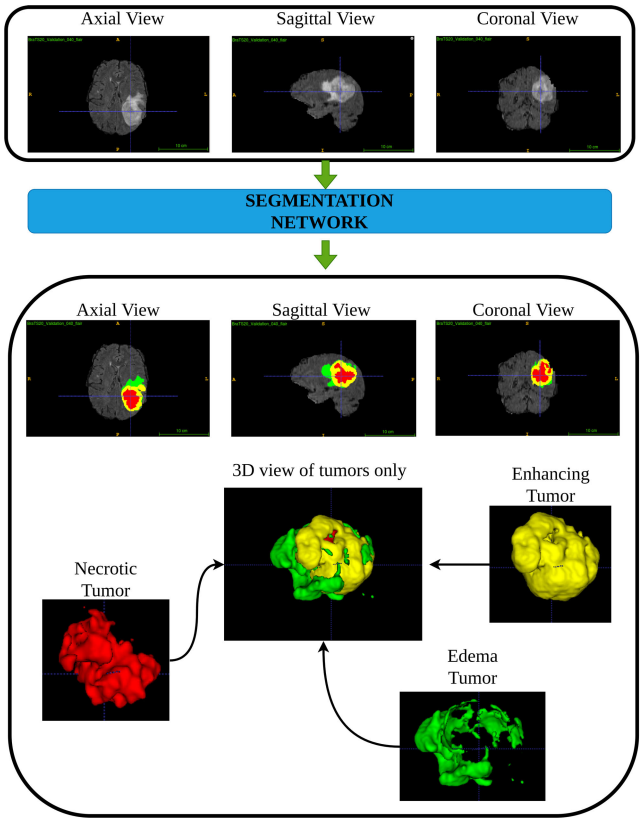


**FIGURE 2.** An overview of tumor segmentation procedure.

### B. SURVIVAL PREDICTION

#### 1) LOCAL SPATIAL RELATIONSHIP AWARENESS FRAMEWORK

Local spatial relationships in this paper are mentioned about the ability to distinguish a couple of two patches are from the same image or not, which indicates intra-local spatial relationships and inter-local spatial relationship awareness. When the model can understand the local spatial relationships, the medical characteristic related to survival prediction will be explored much more under the kind of deep feature information. An image can have multiple local spatial areas, including helpful medical characteristics information. Especially in some previous research, the surrounding region of the tumor is proven that have meaning for survival prediction in GBM because it contains the peritumoral area containing critical information, such as the growing tumor, surrounding mass effect, the status of tumor contact with the ventricle [2], [3], [4], [5], [6], [7] and stromal cells that promote GBM growth and invasion [8]. With this inspiration, the proposed framework is partially based on a self-supervised learning approach, with the pretext task being local context contrastive learning. Using that way, the local spatial of the image is exploited well under robust image-based feature representation. Suppose that the model can distinguish a couple of two image patches from the same image or not. It means that the model could be deeply understood in the brain image structure. Inside the brain structure, several meaningful areas prove it correlates with survival prediction factors likes we already mentioned above.

An unlabeled dataset $U$ can be defined as $U = \{a_n\}_{n=1}^{N}$. A backbone B is used to train dataset $U$. We then get the

vector of learnable weights $\omega$. A non-linear function $g_\omega$ has been parameterized by vector $\omega$. To generate meaningful latent features include the local relationship information, through the $g_\omega$, image $a_n$ will become the $m_n$ (latent feature, $g_\omega(a_n) = m_n$). From dataset $U$, we will have a set $M = \{m_n\}_{n=1}^{N}$. During training we also apply an augmentation technique. Particularly, $U^i = \left\{a_n^{(i)}\right\}_{n=1}^{N}$ with i-th set of random augmentations in total samples. Subsequently, $m_n^{(i)}$ can be shows in $M^i = \left\{m_n^{(i)}\right\}_{n=1}^{N}$. Suppose that K represents the total number of augmentations $U^1, \ldots, U^A$ and their latent features can be represented as $M^1, \ldots, M^A$. We employ a relation network [39] as a local spatial relationship awareness network (LSRAN) $sra_\phi$ for a binary classification network to classify whether or not a pair of latent features is from the same image. In these cases, the network has knowledge about intra local spatial relationships and inter local spatial relationships. The output put of the LSRAN network is a relation score, $h$. The complete learning objective function ($CLOF$) can be shown as follows:

$$\begin{aligned} CLOF &= \underset{\theta,\phi}{argmin} \sum_{n=1}^{N}\sum_{i=1}^{A}\sum_{j=1}^{A}(Loss_{same\ image} \\ &\quad + Loss_{different\ image}) \\ &= \underset{\theta,\phi}{argmin} \sum_{n=1}^{N}\sum_{i=1}^{A}\sum_{j=1}^{A} \\ &(Loss(sra_\phi(concat(z_n^i, z_n^j)), t = 1) \\ &\quad + Loss(sra_\phi(concat(z_n^i, z_{/n}^j)), t = 0). \end{aligned} \tag{1}$$

Because we use the Focal loss function for binary classification, therefore loss function can be defined in form as below:

$$L_{focal} = -\sum_{n=1}^{P=2}(1 - h_n)^\lambda t_n log(h_n). \tag{2}$$

### 2) SURVIVAL CLASSIFICATION BASED ON 2D IMAGE

We proposed a classification model which consists of a spatial learned backbone with two fully connected (FC) layers. The first FC layers incorporate the Batch Normalization [40] layer with ReLU activation. This model predicts the class of survivors in each slice image. Our results achieved a competitive performance in accuracy metric with an accuracy of 0.517 and very high performance in SpearmanR correlation of 0.459 on the BraTS 2020 [41], [42], [43] dataset validation sets. Figure 2 illustrates our overall architecture with the segmentation and the survival classification frameworks. We used a cross entropy loss $L_{ce}$ function for the survivor classification task. The objective loss function can be presented as follows:

$$L_{ce} = -\sum_{n}^{P} t_n log(h_n). \tag{3}$$

#### *a: FROM 2D RESULTS TO 3D RESULTS VIA MAJOR VOTING*

From the results of classification using 2D axial images, we applied a majority voting technique to decide the survivor class for patient survival classification. Each patient was classified into one of three classes: short survivor, mid-survivor, or long survivor. To facilitate result submission to the BraTS organizers website, if the patient belonged to the short survivor class, we assigned the patient's overall survival days as 150. Similarly, the mid-survivor was 375, and 525 days for the long survivor.

#### *b: GLOBAL STRUCTURE AWARENESS FROM FLAIR MRI*

Global structure awareness is the ability of the proposed model can reconstruct a whole image based on an input image. After training the model with the same input and output, we use this pretrained weight to extract the feature and concatenate them with local spatial relationships features and radiomics features to get the final prediction in survival days. From the introduction, disruptions in the normal-appearing brain beyond the lesion could affect patient survival. These disruptions are related to post-stroke depression and the outcome of survival prediction in glioblastoma patients [10], [11]. The status of glioblastoma has been found to impact global brain function, including communication between brain regions far from the tumor [12]. Previous research has investigated the spatial distribution of the connectomic profile and found that patients with newly diagnosed gliomas have globally altered functional connectomic profiles that mainly affect hub connectivity and are related to clinical phenotypes. This means that the brain's global structure correlates with survival prediction in glioblastoma patients. Finally, neuroplasticity of structural, topological, biochemical metabolism, and related mechanisms of the brain come through multimodal MRI [13], which may contribute to the improvement of prognosis and function in glioma patients. Based on the valuable global structure information with prognosis in glioblastoma patients, as we mentioned, we employed a global structure awareness network to capture global information from an entire image and then use it for the survival prediction task.

To better capture the global features from FLAIR MRI, we used a Swin Transformer UNet [44] which consists of three modules: Shallow feature extraction, UNet feature extraction, and reconstruction. Because the input and output images are the same, the model can capture better the global structure of the image. Swin Transformer Unet was selected for global structure awareness because it has four advantages compared to others. The first one is high accuracy. The model has achieved state-of-the-art results on several benchmark datasets for semantic segmentation, indicating its high accuracy in predicting pixel-level labels. Next is the scalability characteristic. The Swin Transformer architecture is designed to be scalable, which means that the model can be easily adapted to different input image sizes without sacrificing performance. The third one is flexibility. The UNet

architecture used in Swin Transformer UNet allows for the incorporation of skip connections, which can improve the segmentation accuracy by allowing the model to leverage low-level features from earlier layers. The final advantage is that the Interpretable representations. The Swin Transformer architecture is based on self-attention, which can capture global dependencies between different parts of an image. This means that the model can generate more interpretable representations of the input images and improve its ability to reason about spatial relationships between objects. Overall, Swin Transformer UNet combines the strengths of both Swin Transformer and UNet architectures, resulting in a powerful and efficient model for semantic segmentation tasks. Therefore, Swin Transformer Unet is also suitable for our global structure awareness framework. Basically, this is the image reconstruction framework. We utilized the output of the encoder to acquire features from the entire MRI image.

### c: LOW LEVEL FEATURE EXTRACTION

For a FLAIR 2D-axial input image, $I_{FA} \in \mathbb{R}^{H\times W\times 3}$ where H and W are the resolution of the image. A single 3 × 3 convolution layer $Net_{LLE}$ was employed to extract the color or texture information of the input image. The low level feature $Fe_{LL} \in \mathbb{R}^{H\times W\times C}$ can be defined as:

$$Fe_{LL} = Net_{LLE}(I_{FA}) \tag{4}$$

where C is the number of channels for low level features.

### d: DEEP FEATURE EXTRACTION

The extracted low level features $Fe_{LL}$ are fed into the variant of UNet $Net_{HLE}(.)$ to extract the deep feature and multi-scale features $Fe_{HL} \in \mathbb{R}^{H\times W\times C}$:

$$Fe_{HL} = Net_{HLE}(Fe_{LL}) \tag{5}$$

where $Net_{HLE}(.)$ is a variant of UNet architecture integrated Swin Transformer Block (STB). Each block includes eight Swin Transformer Layers inside. The details of the STB and Swin Transformer Layer (STL) are presented in Figure 3.

### e: RECONSTRUCTION MODULE

A 3 × 3 convolution $Net_{Re}(.)$ was employed to generate the reconstructed image $\hat{I}_{FA} \in \mathbb{R}^{H\times W\times 3}$ from deep features $Fe_{HL}$ which is formulated as:

$$\hat{I}_{FA} = Net_{Re}(Fe_{HL}) \tag{6}$$

$I_{FA}$ is obtained by taking the FLAIR 2D-axial image as the input and this is also the ground truth image.

An overall equation of global structure awareness framework can be represented as:

$$\hat{I}_{FA} = Net_{Re}(Net_{HLE}(Net_{LLE}(I_{FA})) \tag{7}$$

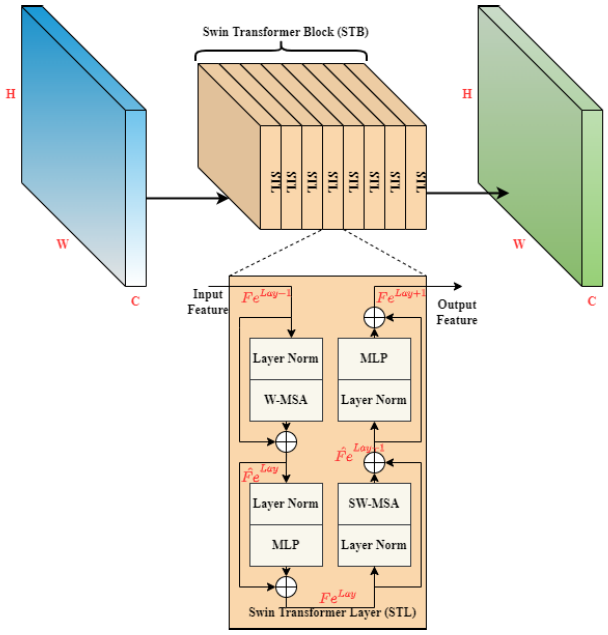


**FIGURE 3.** The detail of swin transformer block and swin transformer layer.

### f: SWIN TRANSFORMER BLOCK

In the deep feature extraction network, we used STB to replace the traditional convolutional layer. Although the original transformer layer has been valuable in the NLP field [45], there are several problems arising from it in computer vision tasks. For example, it is not good at solving dense prediction tasks like reconstruction [46]. Therefore, a new version of transformer, called a swin transformer, was developed to address some disadvantages of the raw transformer layer. The swin transformer is constructed using multiple STLs. An STL is usually made from multiples of two components, in which the first component is a window multi-head self-attention (WMSA) and the rest is a shifted window multi-head self-attention. The feature processing procedure in STL can be represented as:

$$\hat{Fe}^{Lay} = WMSA(LN(Fe^{Lay-1})) + Fe^{Lay-1}, \tag{8}$$

$$Fe^{Lay} = MLP(LN(\hat{Fe}^{Lay})) + \hat{Fe}^{Lay}, \tag{9}$$

$$\hat{Fe}^{Lay+1} = SWMSA(LN(Fe^{Lay})) + Fe^{Lay}, \tag{10}$$

$$Fe^{Lay+1} = MLP(LN(\hat{Fe}^{Lay+1})) + \hat{Fe}^{Lay+1}, \tag{11}$$

where LN(.) denotes Layer Normalization and MLP is multilayer perceptron.

## IV. EXPERIMENTAL RESULTS

### A. EVALUATION METRICS

We evaluated the results by submitting to the challenge website https://ipp.cbica.upenn.edu. Following the rules of the BraTS challenge [1], overall survival days were divided into short-survivor, mid-survivor, and long-survivor classes.

Patients who have survived less than 300 days were assigned to the short-survivor class. Patients who survived longer than 450 days were assigned to the long-survivor class. Patients who survived between 300 days and 450 days were assigned to the mid-survivor class. Additionally, these thresholds were come from statistical consideration of the survival distributions across the complete dataset. Moreover, they chose these thresholds based on equal quantiles from the median OS (approximately 12.5 months) to avoid potential bias towards one of the survival groups (short- vs long- survivors) and while considering that discrimination of groups should be clinically meaningful [1]. The *SpearmanR*, *Accuracy* and *MSE* metrics were employed to evaluate the performance of the survival prediction task.

The equation of *Accuracy* metric is defined as follows:

$$Accuracy = \frac{correct\ predictions}{total\ predictions} \tag{12}$$

*SpearmanR* was the correlation metric used in survival prediction tasks and the equation is presented by:

$$SpearmanR = 1 - 6\frac{\sum (R - R^*)^2}{N(N^2 - 1)} \tag{13}$$

where $N$ is denoted the number of samples, the rank of predicted value $R$ and the rank of ground truth $R^*$.

The mean squared error metric *MSE* was used to compute the difference between our overall survival days predicted with the ground truth of each patient. The MSE equation is defined as follows:

$$MSE = \frac{\sum_{i=1}^{s}(d_i - \hat{d}_i)^2}{s} \tag{14}$$

where $s$ is the number of samples and $d_i$ and $\hat{d}_i$ are the predicted overall survival days and the actual survival days of a patient $i$, respectively.

### B. DATASET AND IMPLEMENTATION DETAILS

We used the BraTS 2020 datasets [41], [42], [43] to evaluate our method. The training set data consists of 369 3D MR images with an annotation map for the segmentation phase, while the validation set includes 125 samples without segmented labels. Each subject has a size of 155 × 240 × 240. The annotations for the segmentation task have four values corresponding to four classes: 1 for necrotic tumor, 2 for edema tumor, 4 for enhancing tumor, and 0 for the rest. The number of samples for evaluating the survival prediction task is smaller than those for the segmentation task because the online evaluation web page only focuses on patients whose resection status is gross total resection. We used the PyTorch framework to implement our deep learning-based method during the training and inference phases. Both segmentation and survival classification models were trained on a GPU RTX 3090 with 24GB memory. We first trained the unsupervised models LSRAN to obtain the local spatial relationships learned backbone, then utilized this backbone to train the supervised survivor classification model. We set the learning rate to 0.001, the epochs to 250, and the batch size to 64 to optimize the model. Table 2 shows the comparisons of the SpearmanR and Accuracy performances with other published methods on the BraTS 2020 validation dataset, while Table 2 presents a comparison of the SpearmanR performances with other published methods on the BraTS 2019 and BraTS 2018 validation datasets. From the experimental results, the FLAIR modality showed the highest correlation with the survival prediction output with a correlation SpearmanR of 0.459. The Figure 5 A and Figure 5 B present comparisons of SpearmanR and Accuracy performances between using our FLAIR modality and other modalities, combination approaches on the BraTS 2020 validation dataset. In the segmentation phase, our segmented results achieved a dice score of 0.89845 in the whole tumor, 0.77734 in the tumor core, and 0.78957 in the enhancing tumor.

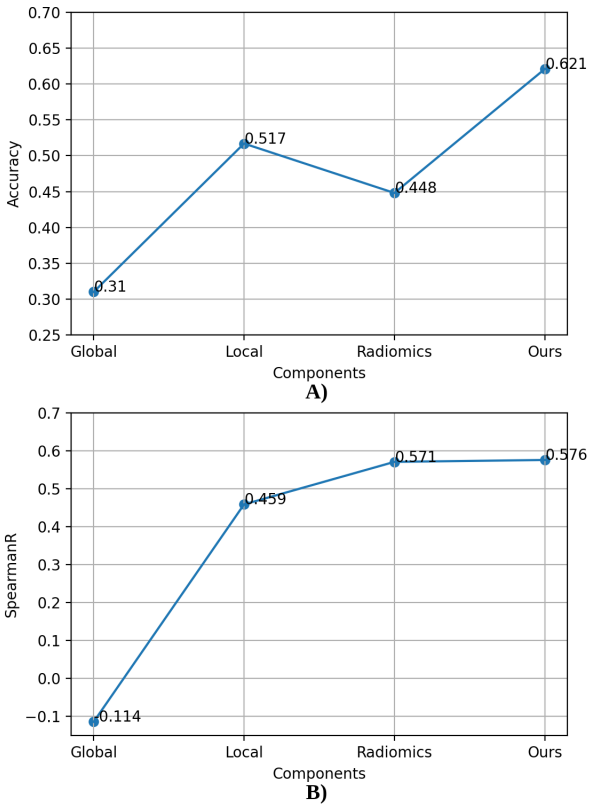


**FIGURE 4. Effect of each local, global and radiomics features on survival prediction.**

### C. ABLATION STUDIES

We performed ablation studies to investigate the role of each component of our approach. We first used only local spatial information for survival prediction. Then, we used only radiomics features for survival prediction. We also used only global structure information for survival prediction. Next, we used local, global, and radiomics feature for survival prediction. Because we wanted to understand the radiomics features, we applied feature selection using a C-index.

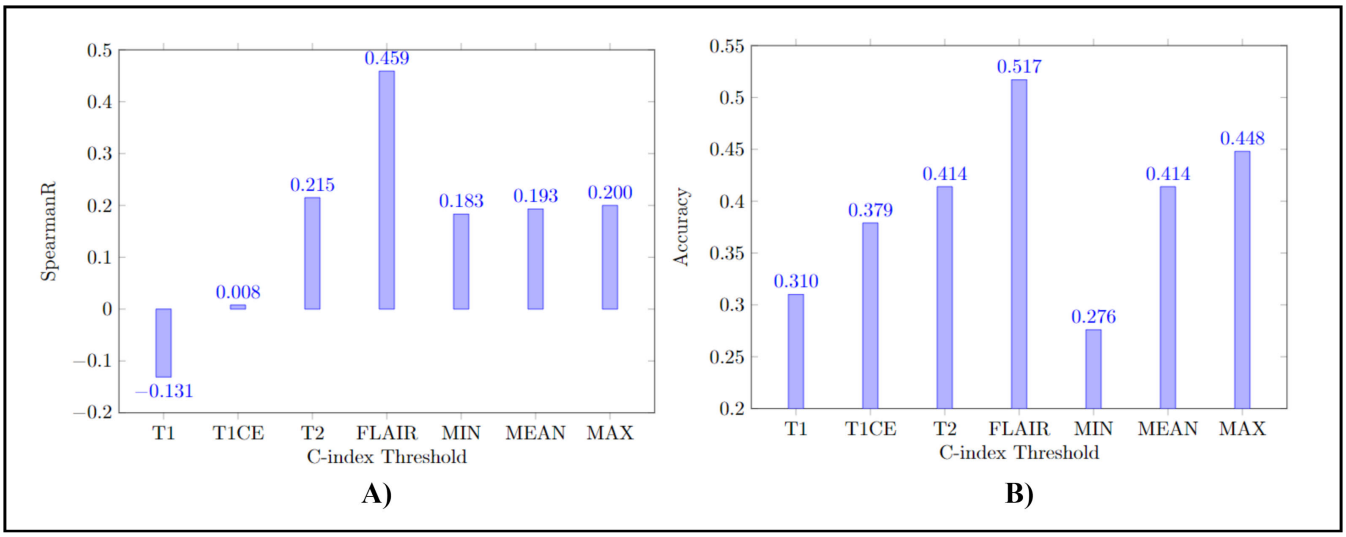


**FIGURE 5.** Effect of modality on survival prediction.

**TABLE 2.** Comparison of SpearmanR and Accuracy performances between our local spatial relationships approach to other published methods on the BraTS 2020 validation dataset.

| Method | SpearmanR | Accuracy |
|---|---|---|
| [24] | 0.123 | 0.345 |
| [26] | 0.134 | 0.483 |
| [27] | 0.134 | 0.517 |
| [28] | 0.217 | 0.517 |
| [29] | 0.228 | 0.414 |
| [30] | 0.249 | 0.517 |
| [25] | 0.253 | 0.414 |
| [31] | 0.280 | 0.450 |
| **Ours** | 0.459 | 0.517 |

**TABLE 3.** Comparison of SpearmanR and Accuracy performances to other published methods on the BraTS 2020 validation dataset.

| Method | Accuracy | MSE | SpearmanR |
|---|---|---|---|
| [24] | 0.345 | 149,764.866 | 0.123 |
| [32] | 0.379 | 93,859.536 | 0.280 |
| [29] | 0.414 | 101,278.000 | 0.228 |
| [25] | 0.414 | 98,704.655 | 0.253 |
| [31] | 0.450 | 109,564.000 | 0.280 |
| [26] | 0.483 | 105,079.421 | 0.134 |
| [28] | 0.517 | 116,083.477 | 0.217 |
| [30] | 0.517 | 97,777.080 | 0.249 |
| [27] | 0.517 | 122,515.761 | 0.134 |
| Ours | 0.621 | 97,216.345 | 0.576 |

To evaluate the performance of each kind of medical image, we used several types of images, to observe the correlation between image category and survival. Finally, we performed the experiment using multiple machine learning approaches to find the best for our framework.

### 1) EFFECT OF THE LOCAL, GLOBAL, AND RADIOMICS FEATURES ON OUR SURVIVAL PREDICTION FRAMEWORK

When we used a combination of global, local, and radiomics features, we achieved the best results. When we used only global context, the results were worst because the global features are mainly extracted from typical areas of the brain, which do not significantly affect survival results. The ratio of normal areas to tumor areas is high. Although using only radiomics features achieved high performance according to the correlation metric, the accuracy was low. Figure 4 shows that our proposed method which combines local, global and radiomics features achieved the best results compared to others.

### 2) EFFECT OF THE MEDICAL IMAGE MODALITY ON OUR SURVIVAL PREDICTION FRAMEWORK

The proposed method uses local and global features from FLAIR MR images. However, we also considered other kinds of modalities in MR images, such as T1, T1ce, T2, and the combination of four modalities. In Figure 5, the FLAIR image is shown to have the best correlation with survival prediction results. We achieved a Spearman R of 0.459 and Accuracy of 0.517. Those results are from the local spatial relationship framework.

### 3) THE EFFECTS OF RADIOMIC FEATURES ON OUR SURVIVAL PREDICTION FRAMEWORK

We further explored the relationship between the number of radiomics and model performance in Figure 6. From four modalities of medical images, T1. T1ce, and FLAIR, we extracted a total of 1284 radiomics features. Using all radiomics features, we achieved an accuracy of 0.483 and a Spearman R of 0.459. Given that these results were not particularly good, we used the C-index metric to identify only high correlation features. From Figure 6, we can see that when we chose a threshold of the C-index of 0.585, there were only six highly correlated features, producing an accuracy of 0.621, Spearman R of 0.576 and MSE of 97216.345.

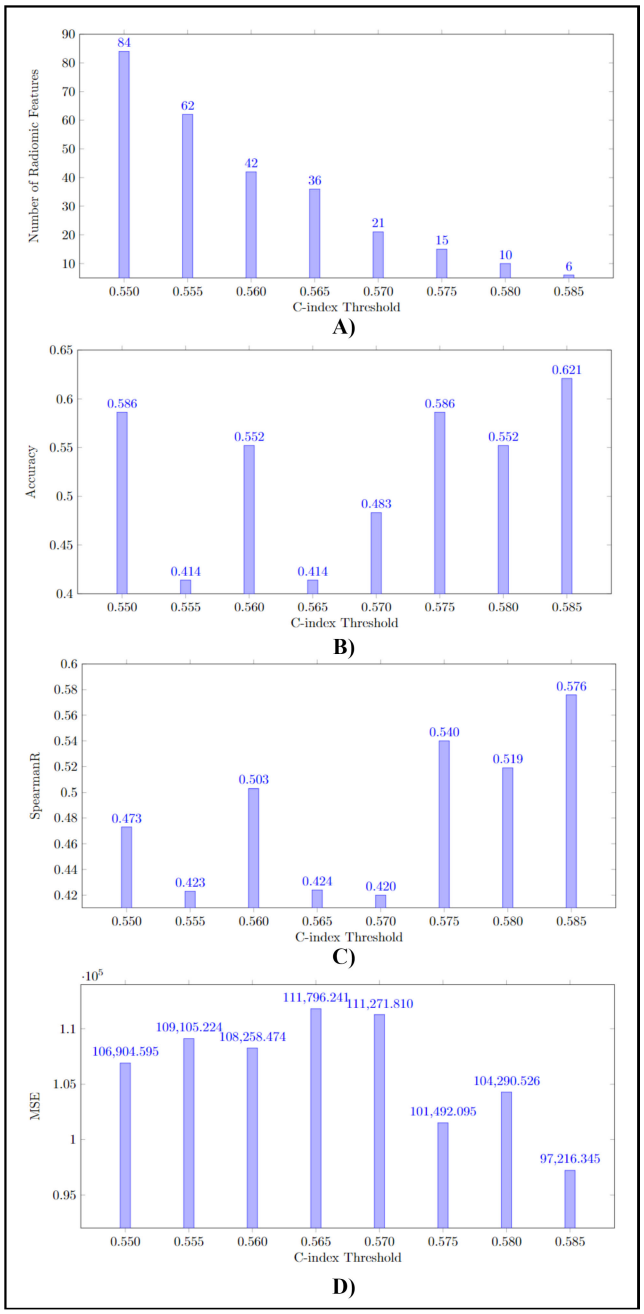


**FIGURE 6.** Effect of number of radiomics features on survival prediction.

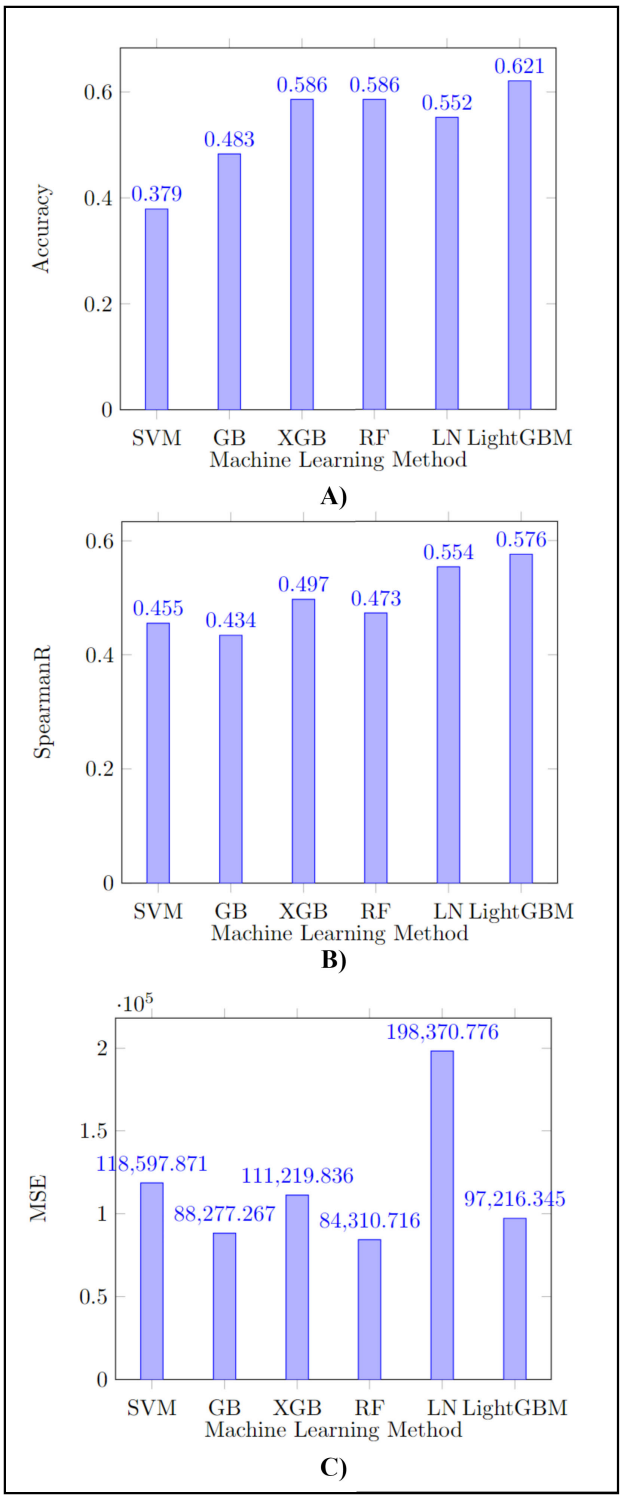


**FIGURE 7.** Effect of machine learning approach on survival prediction.

#### 4) EFFECT OF MACHINE LEARNING METHODS ON OUR SURVIVAL PREDICTION FRAMEWORK

We experimented with many kinds of machine learning algorithms to find the one best suited to our extracted features. Figure 7 shows that the Light GBM method produced the best result overall, with the highest accuracy and Spearman R. Although Random Forest produced a low MSE, the Accuracy and Spearman R metrics were not good. We selected the Light GBM method, to produce the best Accuracy and Spearman R.

### D. DISCUSSION

In this section, we discuss the results of experiments on the use of different features in MR images to predict survival outcomes in patients with glioblastoma. The best results were

achieved by combining global, local, and radiomics features. Using only global context was the worst, as it mainly relies on typical brain areas which do not have a significant impact on survival. The use of only radiomics features showed high correlation but low accuracy. The experiments also explored different modalities in MR images and found that the combination of local and global features from FLAIR MR images performed the best in terms of accuracy and correlation metrics. The study further investigated the relationship between the number of radiomics features and model performance and found that using a feature selection approach to choose the most highly correlated radiomics features instead of using all of them improved accuracy. When a threshold of 0.585 for the C-index correlation was used, only six features were selected, resulting in an accuracy of 0.621, a Spearman R of 0.576, and an MSE of 97216.345. Additionally, there are several good research on survival that achieve high accuracies that we can discuss more in detail and can help us have a deep understanding in the context of a broader range of methods than just the BRATS analysis. Di Noia's paper [47] provides an overview of the current state-of-the-art AI techniques applied to MRI for predicting survival in brain tumor patients. Some studies have claimed up to 98% accuracy, but these results should be taken with caution as they may not apply to all patients or situations. The accuracy of AI models can be impacted by factors such as data quality and quantity, evaluation methods, and patient population. The paper by Di Noia employed ten-fold cross-validation and achieved 98% accuracy in classifying high- and low-risk patients. Sanghani's paper [48] used cross-validation but did not use private validation data. Our paper is different as we used a three-class classification, and the results come from the official BraTS challenge website. We aim to demonstrate that our method is effective for both training and private validation datasets. In Palsson's paper [49], the authors used MRI data to automatically segment the whole brain and tumor and train a machine learning model for predicting survival in glioblastoma patients. The study results from offer insight into the potential of using MRI data and machine learning for survival prediction, but the 0.631 value reported is not the accuracy of a three-class classification but rather the C-index calculated for the training set evaluation. We also showed our training results on C-index and SpearmanR metrics in Fig 8. This figure illustrates training results in C-index and SpearmanR metrics between different kinds of regressors. Finally we can see the LighGBM generated the best results.

Suter's paper [50] investigates the use of radiomics and MRI data for predicting survival in glioblastoma patients. The authors extract radiomic features from MRI data and use these to train machine learning models for survival prediction. The results offer insight into the potential of radiomics and MRI data for survival prediction, but it is unclear which public dataset was used. McKinley's paper [25] reports an accuracy of 0.61 from the evaluation of the test set, which is not currently available. Ref. 38 is the paper of Mc Kinley, who is the winner of BraTS 2020 survival prediction challenge. Our results have been compared to the first prize winner of the BraTS 2020 survival prediction challenge and we outperform them, with an accuracy of 0.621 and a SpearmanR of 0.576 in the validation set, while they had 0.414 in accuracy metric and a SpearmanR of 0.253.

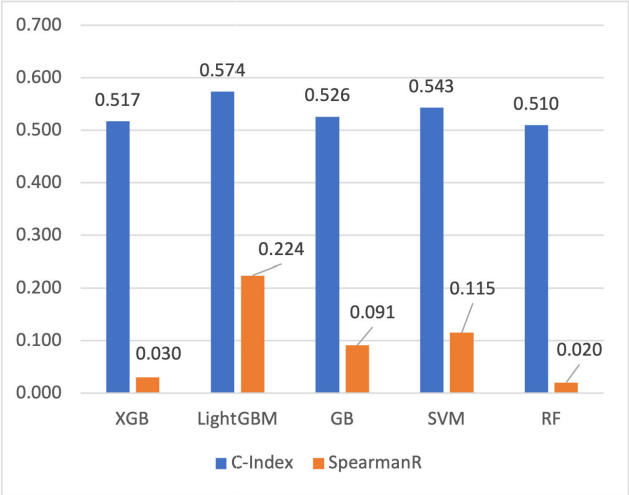


**FIGURE 8.** The illustration of training results in C-index and SpearmanR metrics between different kinds of regressors.

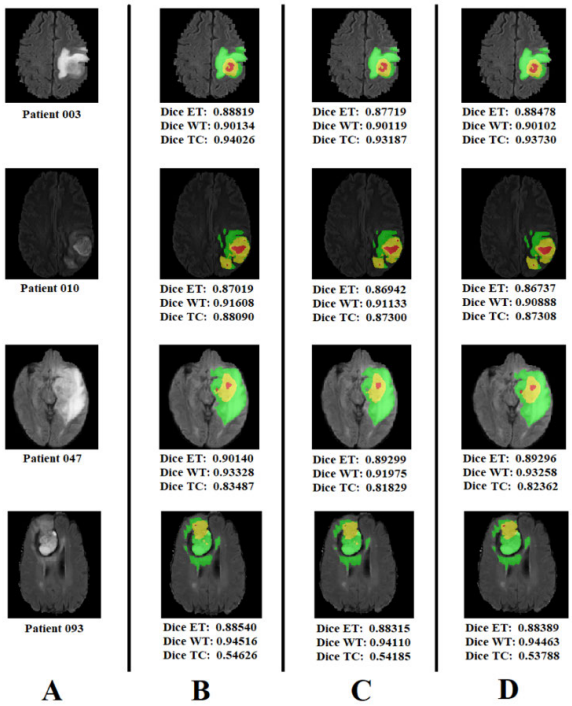


**FIGURE 9.** Example images with qualitative results of tumor segmentation. in different segmentation methods. (A) column is the input images, (B) column is our segmented results, (C) column is the segmented results from DKNet, (D) column is the segmented results from DMFNet.

## V. CONCLUSION

Our paper proposes a framework that utilizes deep feature information to predict survivor class in brain tumor patients using FLAIR MRI data. We focus on capturing local spatial relationships to capture critical medical characteristics related to survival prediction, such as the growing tumor, surrounding mass effect, and tumor contact with the ventricle and stromal cells that promote GBM growth and invasion. We also recognize the importance of global brain structures in survival prediction and use a global structure awareness network to capture global information from the entire image. Our study shows that combining local and global information in FLAIR images can improve the prediction of survival in brain tumor patients, specifically those with glioblastoma. Our proposed framework achieves a superior accuracy metric of 0.621. We not only got good results in the accuracy metric but also had the best correlation score of 0.576, represented by the SpearmanR metric. In experimental results, we conduct a comparison with other recent research, and it shows the effectiveness of our approach. This research can assist doctors and oncologists in planning treatment for brain tumor patients. For further research, we suggest investigating the use of other imaging modalities, such as diffusion-weighted imaging and perfusion-weighted imaging, and combining them with FLAIR MRI data to improve the accuracy of survival prediction. Additionally, exploring the use of other deep learning models, such as transformer-based models, and incorporating clinical and genetic information into the model could be a promising direction for future research. Finally, conducting a large-scale multi-center study to validate the effectiveness of our proposed framework would be beneficial in the clinical setting.

## REFERENCES

[1] S. Bakas, "Identifying the best machine learning algorithms for brain tumor segmentation, progression assessment, and overall survival prediction in the BRATS challenge," 2018, *arXiv:1811.02629*.

[2] C.-X. Wu, G.-S. Lin, Z.-X. Lin, J.-D. Zhang, S.-Y. Liu, and C.-F. Zhou, "Peritumoral edema shown by MRI predicts poor clinical outcome in glioblastoma," *World J. Surgical Oncol.*, vol. 13, no. 1, pp. 1–9, Dec. 2015.

[3] B. R. J. van Dijken, P. Jan van Laar, C. Li, J.-L. Yan, N. R. Boonzaier, S. J. Price, and A. van der Hoorn, "Ventricle contact is associated with lower survival and increased peritumoral perfusion in glioblastoma," *J. Neurosurg.*, vol. 131, no. 3, pp. 717–723, Sep. 2019.

[4] C.-X. Wu, G.-S. Lin, Z.-X. Lin, J.-D. Zhang, L. Chen, S.-Y. Liu, W.-L. Tang, X.-X. Qiu, and C.-F. Zhou, "Peritumoral edema on magnetic resonance imaging predicts a poor clinical outcome in malignant glioma," *Oncol. Lett.*, vol. 10, no. 5, pp. 2769–2776, Nov. 2015.

[5] S. Rathore, H. Akbari, and J. Doshi, "Radiomic signature of infiltration in peritumoral edema predicts subsequent recurrence in glioblastoma: Implications for personalized radiotherapy planning," *J. Med. Imag.*, vol. 5, no. 2, Mar. 2018, Art. no. 021219.

[6] P. Prasanna, J. Mitra, N. Beig, A. Nayate, J. Patel, S. Ghose, R. Thawani, S. Partovi, A. Madabhushi, and P. Tiwari, "Mass effect deformation heterogeneity (MEDH) on gadolinium-contrast T1-weighted MRI is associated with decreased survival in patients with right cerebral hemisphere glioblastoma: A feasibility study," *Sci. Rep.*, vol. 9, no. 1, p. 1145, Feb. 2019.

[7] K. Schoenegger, S. Oberndorfer, B. Wuschitz, W. Struhal, J. Hainfellner, D. Prayer, H. Heinzl, H. Lahrmann, C. Marosi, and W. Grisold, "Peritumoral edema on MRI at initial diagnosis: An independent prognostic factor for glioblastoma?" *Eur. J. Neurol.*, vol. 16, no. 7, pp. 874–878, Jul. 2009.

[8] J.-M. Lemée, A. Clavreul, and P. Menei, "Intratumoral heterogeneity in glioblastoma: Don't forget the peritumoral brain zone," *Neuro-Oncol.*, vol. 17, no. 10, pp. 1322–1332, Oct. 2015.

[9] Y. Wei et al., "Structural connectome quantifies tumor invasion and predicts survival in glioblastoma patients," *Brain*, 2022.

[10] A. Salvalaggio, M. D. F. D. Grazia, M. Zorzi, M. T. de Schotten, and M. Corbetta, "Post-stroke deficit prediction from lesion and indirect structural and functional disconnection," *Brain*, vol. 143, no. 7, pp. 2173–2188, Jul. 2020.

[11] C. Pan, G. Li, P. Jing, G. Chen, W. Sun, J. Miao, Y. Wang, Y. Lan, X. Qiu, X. Zhao, J. Mei, S. Huang, L. Lian, H. Wang, Z. Zhu, and S. Zhu, "Structural disconnection-based prediction of poststroke depression," *Transl. Psychiatry*, vol. 12, no. 1, pp. 1–9, Nov. 2022.

[12] J. Derks, A. R. Dirkson, P. C. de Witt Hamer, Q. van Geest, H. E. Hulst, F. Barkhof, P. J. W. Pouwels, J. J. G. Geurts, J. C. Reijneveld, and L. Douw, "Connectomic profile and clinical phenotype in newly diagnosed glioma patients," *NeuroImage, Clin.*, vol. 14, pp. 87–96, Jan. 2017.

[13] K. Lv, X. Cao, R. Wang, P. Du, J. Fu, D. Geng, and J. Zhang, "Neuroplasticity of glioma patients: Brain structure and topological network," *Frontiers Neurol.*, vol. 13, p. 1025, May 2022.

[14] H. Huang, W. Zhang, Y. Fang, J. Hong, S. Su, and X. Lai, "Overall survival prediction for gliomas using a novel compound approach," *Frontiers Oncol.*, vol. 11, Aug. 2021, Art. no. 724191.

[15] X. Feng, N. J. Tustison, S. H. Patel, and C. H. Meyer, "Brain tumor segmentation using an ensemble of 3D U-Nets and overall survival prediction using radiomic features," *Frontiers Comput. Neurosci.*, vol. 14, p. 25, Apr. 2020.

[16] L. Sun, S. Zhang, H. Chen, and L. Luo, "Brain tumor segmentation and survival prediction using multimodal MRI scans with deep learning," *Frontiers Neurosci.*, vol. 13, p. 810, Aug. 2019.

[17] L. Chato and S. Latifi, "Machine learning and radiomic features to predict overall survival time for glioblastoma patients," *J. Personalized Med.*, vol. 11, no. 12, p. 1336, Dec. 2021.

[18] P. Sanghani, A. B. Ti, N. K. K. King, and H. Ren, "Evaluation of tumor shape features for overall survival prognosis in glioblastoma multiforme patients," *Surgical Oncol.*, vol. 29, pp. 178–183, Jun. 2019.

[19] W. Shuo, D. Chengliang, M. Yuanhan, G. Y. A. Elsa, and B. Wenjia, "Automatic brain Tumour segmentation and biophysics-guided survival prediction," in *Proc. Int. MICCAI Brainlesion Workshop*, 2019, pp. 61–72.

[20] W. Feifan, J. Runzhou, Z. Liqin, M. Chun, and B. Bharat, "3D U-Net based brain tumor segmentation and survival days prediction," in *Proc. Int. MICCAI Brainlesion Workshop*, 2019, pp. 131–141.

[21] R. J. Gillies, P. E. Kinahan, and H. Hricak, "Radiomics: Images are more than pictures, they are data," *Radiology*, vol. 278, no. 2, pp. 563–577, Feb. 2016.

[22] Y. S. SF and A. H. JWL, "Applications and limitations of radiomic," *Phys. Med. Biol.*, vol. 61, p. R150, Jun. 2016.

[23] K. Virendra, "Radiomics: The process and the challenges," *Magn. Reson. Imag.*, vol. 30, no. 9, pp. 1234–1248, 2012.

[24] A. A. F. C. Subhan and S. Nanik, "Modified mobilenet for patient survival prediction," in *Proc. Int. MICCAI Brainlesion Workshop*, 2020, pp. 374–387.

[25] H. Richard, R. Micheal, D. Katrin, M. Raphael, R. Piotr, and W. Roland, "Uncertainty-driven refinement of tumor-core segmentation using 3D-to-2D networks with label uncertainty," in *Proc. Int. MICCAI Brainlesion Workshop*, 2020, pp. 401–411.

[26] A. M. Junaid, A. M. Tahir, S. Hira, R. Basit, and S. A. Raza, "Glioma segmentation using ensemble of 2D/3D U-Nets and survival prediction using multiple features fusion," in *Proc. Int. MICCAI Brainlesion Workshop*, 2020, pp. 189–199.

[27] M. A. Jaime and M.-L. S. Alfonso, "MRI brain tumor segmentation using a 2D-3D U-Net ensemble," in *Proc. Int. MICCAI Brainlesion Workshop*, 2020, pp. 354–366.

[28] A. Rupal and R. Mehul, "Brain tumor segmentation and survival prediction," in *Proc. Int. MICCAI Brainlesion Workshop*, 2019, pp. 338–348.

[29] P. Bhavesh and P. Mehul, "Brain tumor segmentation and survival prediction using patch based modified 3D U-Net," in *Proc. Int. MICCAI Brainlesion Workshop*, 2020, pp. 398–409.

[30] M. Radu, A. Ramona, and B. Mihaela, "A two-stage atrous convolution neural network for brain tumor segmentation and survival prediction," in *Proc. Int. MICCAI Brainlesion Workshop*, 2020, pp. 290–299.

[31] S. Mohammadreza, P. Tony, and P. Michae, "Efficient MRI brain tumor segmentation using multi-resolution encoder–decoder networks," in *Proc. Int. MICCAI Brainlesion Workshop*, 2020, pp. 30–39.
[32] V. L. Bommineni, "PieceNet: A redundant UNet ensemble," in *Proc. Int. MICCAI Brainlesion Workshop*, 2020, pp. 331–341.
[33] M.-T. Tran, T.-B.-T. Do, and G.-S. Lee, "Survivor class prediction by local spatial relationship in FLAIR MRI brain images," in *Proc. Int. Conf. Multimedia Inf. Technol. Appl.*, 2022, pp. 1–4.
[34] S. Roy, D. Bhattacharyya, S. K. Bandyopadhyay, and T.-H. Kim, "An iterative implementation of level set for precise segmentation of brain tissues and abnormality detection from MR images," *IETE J. Res.*, vol. 63, no. 6, pp. 769–783, Nov. 2017.
[35] S. Roy and S. K. Bandyopadhyay, "A new method of brain tissues segmentation from MRI with accuracy estimation," *Proc. Comput. Sci.*, vol. 85, pp. 362–369, Jan. 2016.
[36] S. Roy, T. Meena, and S.-J. Lim, "Demystifying supervised learning in healthcare 4.0: A new reality of transforming diagnostic medicine," *Diagnostics*, vol. 12, no. 10, p. 2549, Oct. 2022.
[37] C. Chen, L. Xiaopeng, D. Meng, Z. Junfeng, and L. Jiangyun, "3D dilated multi-fiber network for real-time brain tumor segmentation in MRI," in *Proc. Int. Conf. Med. Image Comput. Comput.-Assist. Intervent*, 2019, pp. 184–192.
[38] D.-K. Ngo, M.-T. Tran, S.-H. Kim, H.-J. Yang, and G.-S. Lee, "Multi-task learning for small brain tumor segmentation from MRI," *Appl. Sci.*, vol. 10, no. 21, p. 7790, Nov. 2020.
[39] M. Patacchiola and A. Storkey, "Self-supervised relational reasoning for representation learning," 2020, *arXiv:2006.05849*.
[40] I. Sergey and S. Christian, "Batch normalization: Accelerating deep network training by reducing internal covariate shift," in *Proc. Int. Conf. Mach. Learn.*, 2015, pp. 448–456.
[41] S. Bakas, H. Akbari, A. Sotiras, M. Bilello, M. Rozycki, J. Kirby, J. Freymann, K. Farahani, and C. Davatzikos, "Segmentation labels and radiomic features for the pre-operative scans of the TCGA-LGG collection," *Cancer Imag. Arch.*, vol. 286, Jul. 2017.
[42] S. Bakas, H. Akbari, A. Sotiras, M. Bilello, M. Rozycki, J. S. Kirby, J. B. Freymann, K. Farahani, and C. Davatzikos, "Advancing the cancer genome atlas glioma MRI collections with expert segmentation labels and radiomic features," *Sci. Data*, vol. 4, no. 1, pp. 1–13, Sep. 2017.
[43] B. H. Menze, A. Jakab, S. Bauer, J. Kalpathy-Cramer, K. Farahani, J. Kirby, Y. Burren, N. Porz, J. Slotboom, R. Wiest, and L. Lanczi, "The multimodal brain tumor image segmentation benchmark (BRATS)," *IEEE Trans. Med. Imag.*, vol. 34, no. 10, pp. 1993–2024, Oct. 2015.
[44] C.-M. Fan, T.-J. Liu, and K.-H. Liu, "SUNet: Swin transformer UNet for image denoising," 2022, *arXiv:2202.14009*.
[45] V. Ashish et al., "Attention is all you need," in *Proc. Adv. Neural Inf. Process. Syst.*, vol. 30, 2017.
[46] S. Liu, L. Qi, H. Qin, J. Shi, and J. Jia, "Path aggregation network for instance segmentation," in *Proc. IEEE/CVF Conf. Comput. Vis. Pattern Recognit.*, Jun. 2018, pp. 8759–8768.
[47] C. di Noia, J. T. Grist, F. Riemer, M. Lyasheva, M. Fabozzi, M. Castelli, R. Lodi, C. Tonon, L. Rundo, and F. Zaccagna, "Predicting survival in patients with brain tumors: Current state-of-the-art of AI methods applied to MRI," *Diagnostics*, vol. 12, no. 9, p. 2125, Sep. 2022.
[48] P. Sanghani, B. T. Ang, N. K. K. King, and H. Ren, "Overall survival prediction in glioblastoma multiforme patients from volumetric, shape and texture features using machine learning," *Surgical Oncol.*, vol. 27, no. 4, pp. 709–714, Dec. 2018.
[49] S. Pálsson, S. Cerri, H. S. Poulsen, T. Urup, I. Law, and K. Van Leemput, "Predicting survival of glioblastoma from automatic whole-brain and tumor segmentation of MR images," *Sci. Rep.*, vol. 12, no. 1, Nov. 2022, Art. no. 19744.
[50] Y. Suter, U. Knecht, M. Alão, W. Valenzuela, E. Hewer, P. Schucht, R. Wiest, and M. Reyes, "Radiomics for glioblastoma survival analysis in pre-operative MRI: Exploring feature robustness, class boundaries, and machine learning techniques," *Cancer Imag.*, vol. 20, no. 1, pp. 1–13, Dec. 2020.

**MINH-TRIEU TRAN** received the B.S. degree in electronics and telecommunications engineering from Vietnam Aviation Academy, in 2016, the M.S. degree in electronics engineering from the Ho Chi Minh City University of Technology and Education, in 2018, and the Ph.D. degree in computer science from Chonnam National University, Republic of Korea, in 2022. He is currently a Postdoctoral Researcher with the Department of Artificial Intelligence Convergence, Chonnam National University. His research interests include pattern recognition, document image processing, and medical image processing.

**HYUNG-JEONG YANG** (Member, IEEE) received the B.S., M.S., and Ph.D. degrees from Chonbuk National University, South Korea. She is currently a Professor with the Department of Artificial Intelligence Convergence, Chonnam National University, Gwangju, Republic of Korea. Her main research interests include multimedia data mining, medical data analysis, social network service data mining, and video data understanding.

**SOO-HYUNG KIM** (Member, IEEE) received the B.S. degree in computer engineering from Seoul National University, in 1986, and the M.S. and Ph.D. degrees in computer science from the Korea Advanced Institute of Science and Technology, in 1988 and 1993, respectively. Since 1997, he has been a Professor with the Department of Artificial Intelligence Convergence, Chonnam National University, Republic of Korea. His research interests include pattern recognition, document image processing, medical image processing, and ubiquitous computing.

**GUEE-SANG LEE** (Member, IEEE) received the B.S. degree in electrical engineering and the M.S. degree in computer engineering from Seoul National University, Republic of Korea, in 1980 and 1982, respectively, and the Ph.D. degree in computer science from The Pennsylvania State University, in 1991. He is currently a Professor with the Department of Electronics and Computer Engineering, Chonnam National University, Republic of Korea. His research interests include image processing, computer vision, and video technology.